

RESEARCH ARTICLE | JULY 24 2023

Annealing of blue quantum emitters in carbon-doped hexagonal boron nitride

Yongliang Chen  ; Angus Gale; Karin Yamamura; Jake Horder ; Alexander Condos; Kenji Watanabe ; Takashi Taniguchi ; Milos Toth; Igor Aharonovich  

 Check for updates

Appl. Phys. Lett. 123, 041902 (2023)

<https://doi.org/10.1063/5.0155311>

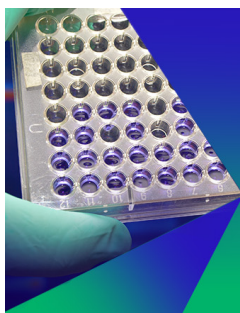


View
Online



Export
Citation

CrossMark



Biomicrofluidics

Special Topic:
Microfluidics and Nanofluidics in **India**

Submit Today



Annealing of blue quantum emitters in carbon-doped hexagonal boron nitride

Cite as: Appl. Phys. Lett. **123**, 041902 (2023); doi: [10.1063/5.0155311](https://doi.org/10.1063/5.0155311)

Submitted: 19 April 2023 · Accepted: 11 July 2023 ·

Published Online: 24 July 2023



View Online



Export Citation



CrossMark

Yongliang Chen,^{1,a)} Angus Gale,¹ Karin Yamamura,^{1,2} Jake Horder,¹ Alexander Condos,¹ Kenji Watanabe,³ Takashi Taniguchi,⁴ Milos Toth,^{1,2} and Igor Aharonovich^{1,2,a)}

AFFILIATIONS

¹School of Mathematical and Physical Sciences, University of Technology Sydney, Ultimo, New South Wales 2007, Australia

²ARC Center of Excellence for Transformative Meta-Optical Systems (TMOS), Faculty of Science, University of Technology Sydney, Ultimo, New South Wales 2007, Australia

³Research Center for Electronic and Optical Materials, National Institute for Materials Science, 1-1 Namiki, Tsukuba 305-0044, Japan

⁴Research Center for Materials Nanoarchitectonics, National Institute for Materials Science, 1-1 Namiki, Tsukuba 305-0044, Japan

^{a)}Authors to whom correspondence should be addressed: yongliang.chen@uts.edu.au and igor.aharonovich@uts.edu.au

ABSTRACT

Reliable methods to create quantum emitters in hexagonal boron nitride (hBN) are highly sought after for scalable applications in quantum photonic devices. Specifically, recent efforts have focused on defects in hBN with a zero phonon line at 2.8 eV (436 nm). Here, we employ carbon-doped hBN crystals that were irradiated by an electron beam to generate these emitters and perform annealing treatments to investigate the stability of the emitters. We find that the blue emitters are stable up to $\sim 800^\circ\text{C}$. However, upon annealing to 1000°C , the emitters disappear, and a family of other emitters appears in the region of hBN that had been irradiated by an electron beam. Our findings contribute to the understanding of emitter species and emitter formation in hBN.

Published under an exclusive license by AIP Publishing. <https://doi.org/10.1063/5.0155311>

Explorations of quantum emitters in solid-state systems are continually expanding, establishing real-world quantum technologies based on single photon emission—including quantum communications and quantum sensing.^{1–3} Recently, hexagonal boron nitride (hBN) has emerged as a compelling solid-state platform for quantum photonics.^{4–7} It hosts a variety of quantum emitters that operate at room temperature and exhibit excellent optical characteristics.^{8–15} Some of the defects also possess favorable spin-photon interfaces addressable by optically detected magnetic resonance (ODMR) spectroscopy.^{16–22}

Recently, a class of quantum emitters in hBN (termed “blue emitters”) has gained attention due to the ability to engineer them on demand with a high degree of spatial precision. Unlike the so-called visible quantum emitters in the red spectral range, the blue emitters have a consistent zero phonon line (ZPL) at $\sim 436\text{ nm}$ and can be engineered deterministically using a focused electron beam.⁵ The emitters have superior optical properties in terms of spectral stability at cryogenic temperature—indeed, subgigahertz linewidths have been reported in a number of studies, as have indistinguishable photons.^{4,5,23–25} While their atomic structure remains unknown, numerous proposals have been put forward, including split interstitial defects.^{5,26,27}

In this work, we study the effect of annealing on the blue emitters. We start with a carbon-doped hBN crystal, with a pronounced defect emission at $\sim 4.1\text{ eV}$ (305 nm) that is known to correlate with a high formation probability of the blue emitters by electron irradiation.^{27,28} We note that the ZPL of this defect shows slightly different values at the range of 300–305 nm (4.07–4.13 eV) and, hence, is commonly referred to as a 4.1 eV defect. Figure 1(a) shows a representative optical image of a carbon-doped hBN crystal.²⁸ To generate blue emitters, several hBN flakes with various thicknesses were exfoliated and irradiated using a scanning electron microscope (SEM). Figure 1(b) shows cathodoluminescence (CL) spectra of a single region before and after electron irradiation. Both spectra show the UV peak at 305 nm, along with phonon replicas at 319 and 334 nm. After electron irradiation, the blue emitters emerge with a ZPL at 436 nm.⁵

To investigate the effects of annealing temperature on blue emitters, a 4×4 array of emitters was fabricated by an electron beam in a carbon-doped hBN flake. The electron beam energy, current, and exposure time per spot were 10 keV, 2.4 nA, and 10 s, respectively. Figure 2(a) shows a confocal map recorded at room temperature using a 405 nm laser. Figure 2(b) shows a representative spectrum of a single quantum emitter acquired from one spot in the array, with a

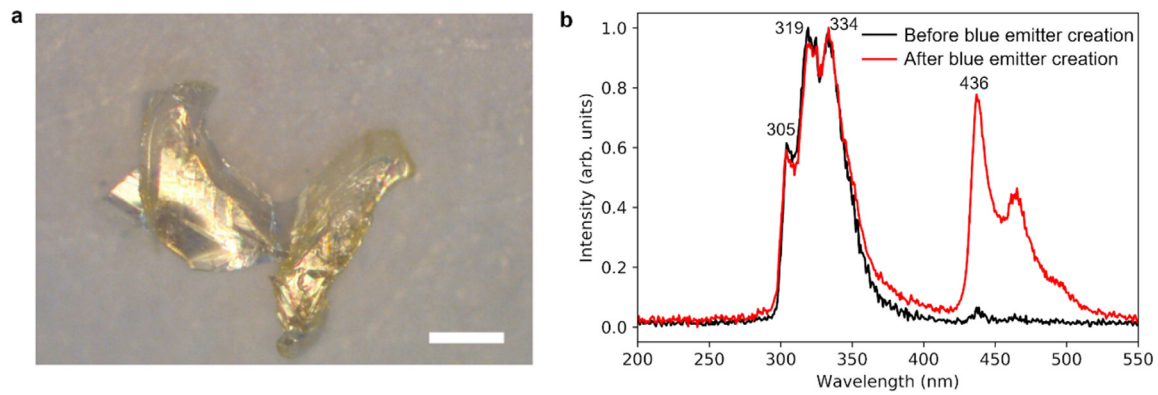


FIG. 1. (a) Optical image of carbon-doped hBN crystals. The scale bar is $200\ \mu\text{m}$. (b) CL spectra from a single region of a carbon-doped hBN flake before and after blue emitter creation by electron beam irradiation.

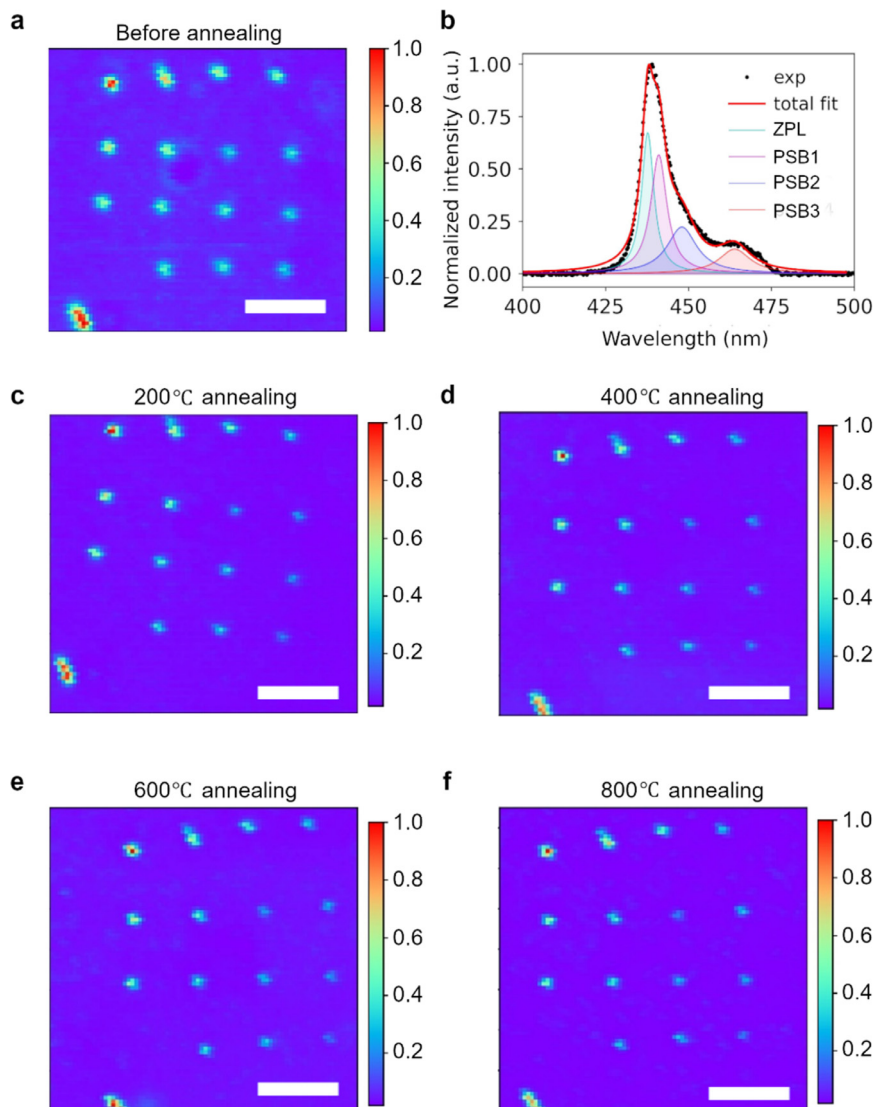


FIG. 2. Annealing of a 4×4 blue emitter array fabricated by electron irradiation of hBN. (a) Confocal map of the emitter array and (b) a corresponding emission spectrum collected from one spot in the array acquired before annealing. (c)–(f) Corresponding confocal maps collected at room temperature after each annealing treatment. The scale bar is $5\ \mu\text{m}$.

characteristic emission at ~ 436 nm, consistent with prior reports.^{5,27} The sample was then placed into a furnace for annealing in 1 Torr of argon. A sequence of one hour annealing treatments was performed at temperatures of 200, 400, 600, 800, and 1000 °C. After each treatment, we collected a confocal map of the array. When the temperature is increased up to 800 °C, no significant change in luminescence was observed, and the array remained intact, as is illustrated in Figs. 2(c)–2(f). Furthermore, no other localized spots (indicative of emitters) were observed in the confocal maps.

To further characterize the effect of the annealing treatments, we fit each spectrum with multi-Lorentzian functions to extract the zero phonon line (ZPL) intensity, position, and full width at half maximum

(FWHM). As shown in Fig. 2(b), fitting reveals four peaks corresponding to a ZPL followed by phonon sidebands (PSBs). Figures 3(a) and 3(d) show the relative ZPL intensity vs annealing temperature. Figures 3(b), 3(e), 3(c), and 3(f) show the change in the ZPL position (ΔZPL) and change in the FWHM ($\Delta FWHM$) relative to their original values prior to annealing at 200 °C. Figures 3(g)–3(i) show the coefficient of variance (the ratio of the fitting uncertainty to the corresponding fitting parameter) of the ZPL intensity, ZPL and FWHM, respectively. The results show that the emissions remained relatively unchanged after the annealing treatments. Notably, none of the emitters disappeared even after annealing at 800 °C. After 800 °C annealing, the larger distribution of intensities and FWHM values and the increased

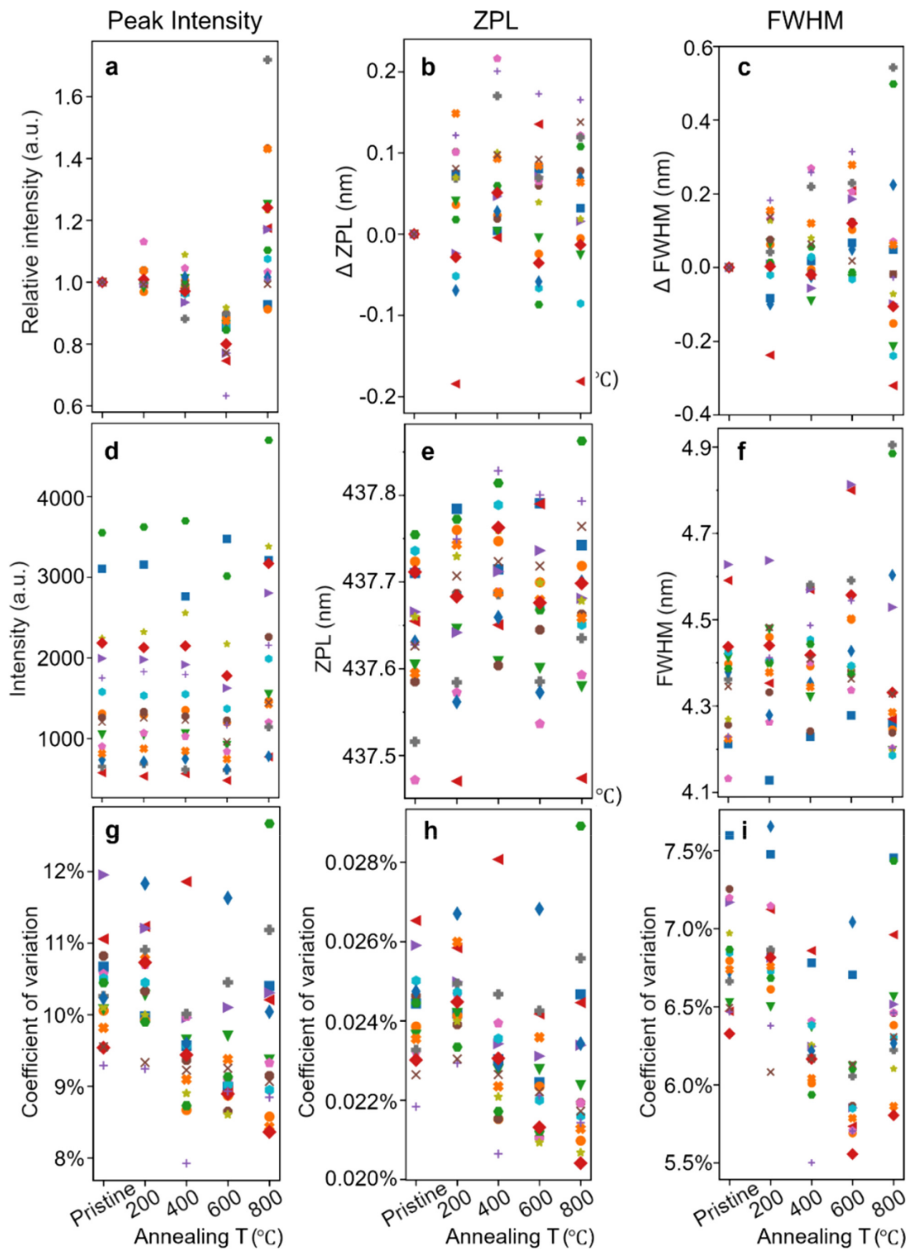


FIG. 3. Effects of annealing treatments on spectral characteristics of the emitters in 16 spots. The change in the relative value [(a)–(c)], the absolute value [(d)–(f)], and the corresponding coefficient of variance [(g)–(i)] of the ZPL intensity, ZPL, and FWHM of each emitter in the array as a function of the annealing temperature. The coefficient of variance is defined as the ratio of fit uncertainties to the corresponding absolute value. The 16 symbols in each figure represent the emitters in the array.

intensity for most emitters are both likely due to an increase in overlapping background luminescence.

However, upon annealing at 1000 °C, the array of blue emitters disappeared and a high density of other randomly distributed emitters appeared in the same area, as is shown by the confocal PL map in Fig. 4(a). Most spots seen in the confocal map correspond to single emitters. We characterized 27 emitters from this area at room temperature using the same excitation conditions as above. The room temperature characteristics of one of these emitters are shown in Figs. 4(b)–4(d). The emitter has a ZPL at 430 nm (~ 2.9 eV) and a phonon sideband at 456 nm (~ 2.7 eV). The emitter stability is illustrated by a time series of spectra acquired over 2 min [Fig. 4(c)], and the photon purity by the second-order autocorrelation function is shown in Fig. 4(d). Figure 4(e) shows a histogram of the ZPL position and FWHM taken from the formed emitters. The FWHM spans ~ 4.5 –10 nm, and the ZPL wavelength distribution spans ~ 420 –480 nm.

Finally, to characterize the formed emitters further, we collected spectra from ten separate emitters at 5 K [Fig. 4(f)]. As the temperature reduces, the ZPL becomes narrower and phonon sideband less pronounced.^{4,23,29} Note that resonant excitation of these emitters was not achieved, likely due to ultrafast spectral diffusion or phonon broadening.

The results in Fig. 3 illustrate that the blue emitters (ZPL position ~ 436 nm) are able to withstand annealing temperatures of up to at least 800 °C, with minimal effects on brightness, ZPL position, and FWHM, and spatial location of the defects in hBN. This emitter has previously been assigned to a split interstitial defect,²⁶ which is consistent with our results. At 1000 °C, the defects responsible for the blue emission either dissociate or re-structure into another configuration. The 1000 °C anneal generates a family of other emitters (Fig. 4) with a ZPL wavelength distribution that is very broad compared to that of the blue emitters. The spatial positions of the generated emitters are not correlated exactly with the original 4×4 blue emitter array, but

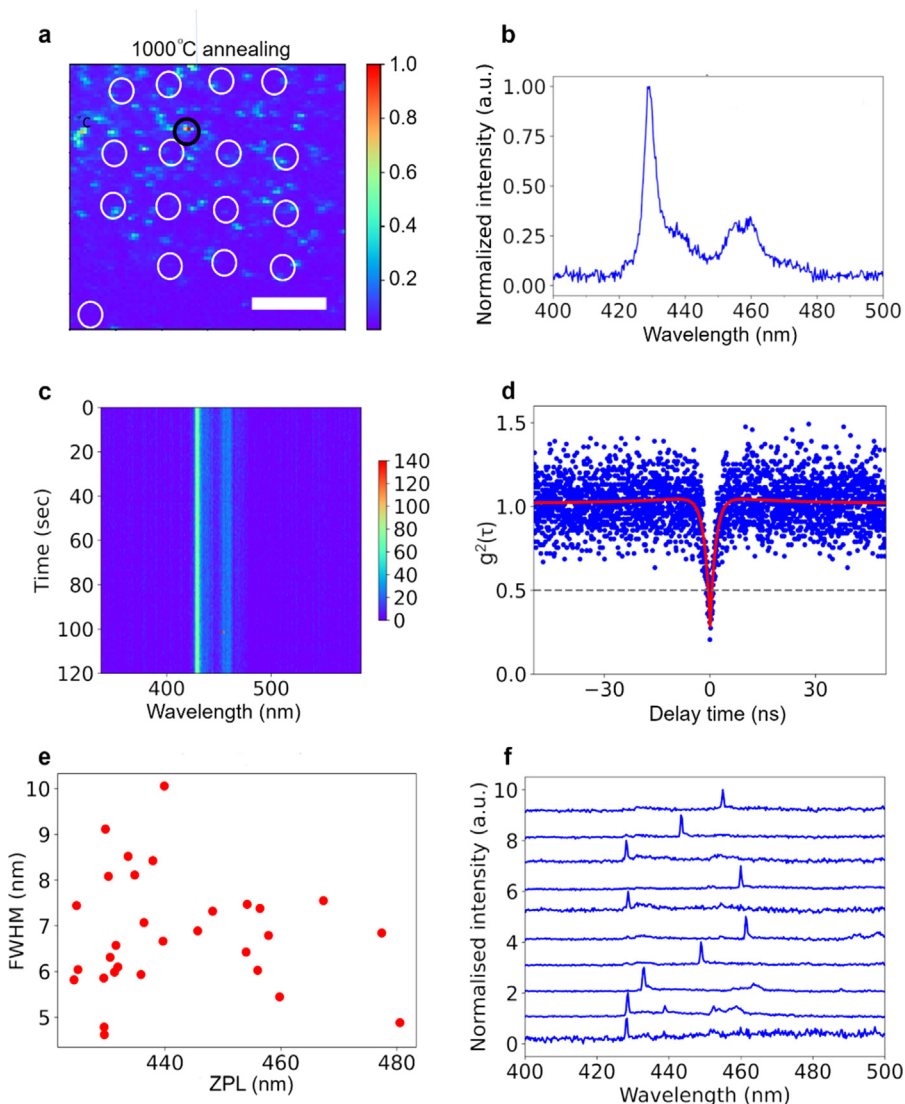


FIG. 4. Optical characterization of the emitters generated by annealing at 1000 °C. (a) Confocal map of the area that contained the original 4×4 array shown in Fig. 2. The white dotted circles indicate the disappeared positions of the original 4×4 array. The scale bar is $5 \mu\text{m}$. (b) PL spectrum of an emitter (black circled-marked position) that formed after annealing at 1000 °C. (c) Spectra vs time, acquired over 2 min to illustrate the spectral stability of the emitter. (d) Second-order autocorrelation function of the emitter. The dip of <0.5 at zero delay time indicates single photon emission. (e) Histogram of the ZPL wavelength and FWHM of the generated emitters. (f) Cryogenic spectra of ten generated emitters collected at 5 K.

they were found only in the general region that contained the array. This indicates that (i) the electron beam irradiation that was used to generate the blue emitter array plays a role in the generation of other emitters upon annealing at 1000 °C, and (ii) defect diffusion takes place at 1000 °C. That is, the formed emitters are generated in a two-step process of electron beam irradiation at room temperature and high-temperature annealing, which gives rise to defect restructuring and diffusion in hBN.

We also note the creation of other emitters at 1000 °C resembles the behavior of the more commonly known carbon-based defects, associated with emission at the red spectral range.^{30–33} The resemblance is in both their emission properties (ZPL and FWHM) as well as in their spectral distribution. Note that since a majority of works focused on hBN quantum emitters excite at 532 nm, the blue spectral range was mostly ignored so far.^{6,34–36} As reported by our previous study, the carbon-doped hBN used in this work would support the existence of carbon-based emitters. Indeed, both annealing and electron irradiation have been shown to activate visible emitters in hBN with ZPLs > 550 nm.^{5,31,32,37}

In conclusion, we investigated the behavior of blue quantum emitters in hBN after various annealing treatments. The emitters are stable up to ~800 °C; however, when the annealing temperature increases to 1000 °C, the blue emitters disappear. Interestingly, at this temperature, a family of other quantum emitters appears, resembling the more commonly known visible emitters. Our studies contribute to the growing understanding of quantum emitters in hBN and their future deployment in quantum applications.

The authors acknowledge financial support from the Australian Research Council (Nos. CE200100010 and FT220100053) and the Office of Naval Research Global (No. N62909-22-1-2028). K.W. and T.T. acknowledge support from the JSPS KAKENHI (Grant Nos. 20H00354, 21H05233, and 23H02052) and World Premier International Research Center Initiative (WPI), MEXT, Japan.

AUTHOR DECLARATIONS

Conflict of Interest

The authors have no conflicts to disclose.

Author Contributions

Yongliang Chen: Data curation (equal); Formal analysis (equal); Investigation (equal); Methodology (equal); Resources (equal); Supervision (equal); Writing – original draft (equal); Writing – review & editing (equal). **Angus Gale:** Data curation (equal); Investigation (equal); Writing – review & editing (equal). **Karin Yamamura:** Data curation (equal); Writing – review & editing (equal). **Jake Horder:** Data curation (equal); Methodology (equal); Writing – review & editing (equal). **Alexander Condos:** Data curation (equal); Investigation (equal); Methodology (equal). **Kenji Watanabe:** Methodology (equal). **Takashi Taniguchi:** Methodology (equal). **Milos Toth:** Writing – review & editing (equal). **Igor Aharonovich:** Supervision (equal); Writing – original draft (equal); Writing – review & editing (equal).

DATA AVAILABILITY

The data that support the findings of this study are available within the article.

REFERENCES

- 1S. Wehner, D. Elkouss, and R. Hanson, *Science* **362**(6412), eaam9288 (2018).
- 2D. D. Awschalom, R. Hanson, J. Wrachtrup, and B. B. Zhou, *Nat. Photonics* **12**(9), 516 (2018).
- 3M. Atatüre, D. Englund, N. Vamivakas, S.-Y. Lee, and J. Wrachtrup, *Nat. Rev. Mater.* **3**(5), 38 (2018).
- 4C. Fournier, S. Roux, K. Watanabe, T. Taniguchi, S. Buil, J. Barjon, J.-P. Hermier, and A. Delteil, [arXiv:2210.05590](https://arxiv.org/abs/2210.05590) (2022).
- 5C. Fournier, A. Plaud, S. Roux, A. Pierret, M. Rosticher, K. Watanabe, T. Taniguchi, S. Buil, X. Quélin, J. Barjon, J.-P. Hermier, and A. Delteil, *Nat. Commun.* **12**(1), 3779 (2021).
- 6H. Akbari, S. Biswas, P. Kumar Jha, J. Wong, B. Vest, and H. A. Atwater, *Nano Lett.* **22**(19), 7798 (2022).
- 7A. Kubanek, *Adv. Quantum Technol.* **5**(9), 2200009 (2022).
- 8L. Gan, D. Zhang, R. Zhang, Q. Zhang, H. Sun, Y. Li, and C.-Z. Ning, *ACS Nano* **16**, 14254 (2022).
- 9X. Xu, Z. O. Martin, D. Sychev, A. S. Lagutchev, Y. P. Chen, T. Taniguchi, K. Watanabe, V. M. Shalaev, and A. Boltasseva, *Nano Lett.* **21**(19), 8182 (2021).
- 10R. Gu, L. Wang, H. Zhu, S. Han, Y. Bai, X. Zhang, B. Li, C. Qin, J. Liu, G. Guo, X. Shan, G. Xiong, J. Gao, C. He, Z. Han, X. Liu, and F. Zhao, *ACS Photonics* **8**, 2912 (2021).
- 11S. Hou, R. Y. Tay, M. D. Birowosuto, P. Coquet, B. K. Tay, S. Umar, H. Wang, M. A. Anicet, and E. H. T. Teo, *2D Mater.* **5**(1), 015010 (2017).
- 12A. Hernández-Minguez, J. Lähnemann, S. Nakhaie, J. M. J. Lopes, and P. V. Santos, *Phys. Rev. Appl.* **10**(4), 044031 (2018).
- 13S. X. Li, T. Ichihara, H. Park, G. He, D. Kozawa, Y. Wen, V. B. Koman, Y. Zeng, M. Kuehne, Z. Yuan, S. Faucher, J. H. Warner, and M. S. Strano, *Commun. Mater.* **4**(1), 19 (2023).
- 14J. Fernandes, T. Queirós, J. Rodrigues, S. S. Nimala, A. P. LaGrow, E. Placidi, P. Alpuim, J. B. Nieder, and A. Capasso, *FlatChem* **33**, 100366 (2022).
- 15W. Liu, Y.-T. Wang, Z.-P. Li, S. Yu, Z.-J. Ke, Y. Meng, J.-S. Tang, C.-F. Li, and G.-C. Guo, *Phys. E Low Dimens. Syst. Nanostruct.* **124**, 114251 (2020).
- 16A. Gottscholl, M. Kianinia, V. Soltamov, S. Orlinskii, G. Mamin, C. Bradac, C. Kasper, K. Krambrock, A. Sperlich, M. Toth, I. Aharonovich, and V. Dyakonov, *Nat. Mater.* **19**(5), 540 (2020).
- 17H. L. Stern, Q. Gu, J. Jarman, S. E. Barker, N. Mendelson, D. Chugh, S. Schott, H. H. Tan, H. Siringhaus, I. Aharonovich, and M. Atatüre, *Nat. Commun.* **13**(1), 618 (2022).
- 18X. Gao, B. Jiang, A. E. L. Allcca, K. Shen, M. A. Sadi, A. B. Solanki, P. Ju, Z. Xu, P. Upadhyaya, Y. P. Chen, S. A. Bhave, and T. Li, *Nano Lett.* **21**(18), 7708 (2021).
- 19A. J. Healey, S. C. Scholten, T. Yang, J. A. Scott, G. J. Abrahams, I. O. Robertson, X. F. Hou, Y. F. Guo, S. Rahman, Y. Lu, M. Kianinia, I. Aharonovich, and J. P. Tetienne, *Nat. Phys.* **19**(1), 87 (2023).
- 20P. Kumar, F. Fabre, A. Durand, T. Clua-Provost, J. Li, J. H. Edgar, N. Rougemaille, J. Coraux, X. Marie, P. Renucci, C. Robert, I. Robert-Philip, B. Gil, G. Cassabois, A. Finco, and V. Jacques, *Phys. Rev. Appl.* **18**(6), L061002 (2022).
- 21N.-J. Guo, W. Liu, Z.-P. Li, Y.-Z. Yang, S. Yu, Y. Meng, Z.-A. Wang, X.-D. Zeng, F.-F. Yan, Q. Li, J.-F. Wang, J.-S. Xu, Y.-T. Wang, J.-S. Tang, C.-F. Li, and G.-C. Guo, *ACS Omega* **7**(2), 1733 (2022).
- 22W. Liu, N.-J. Guo, S. Yu, Y. Meng, Z.-P. Li, Y.-Z. Yang, Z.-A. Wang, X.-D. Zeng, L.-K. Xie, Q. Li, J.-F. Wang, J.-S. Xu, Y.-T. Wang, J.-S. Tang, C.-F. Li, and G.-C. Guo, *Mater. Quantum Technol.* **2**(3), 032002 (2022).
- 23J. Horder, S. J. U. White, A. Gale, C. Li, K. Watanabe, T. Taniguchi, M. Kianinia, I. Aharonovich, and M. Toth, *Phys. Rev. Appl.* **18**(6), 064021 (2022).
- 24I. Zhigulin, K. Yamamura, V. Ivády, A. Gale, J. Horder, C. J. Lobo, M. Kianinia, M. Toth, and I. Aharonovich, *Mater. Quantum Technol.* **3**(1), 015002 (2023).
- 25B. Shevitski, S. M. Gilbert, C. T. Chen, C. Kastl, E. S. Barnard, E. Wong, D. F. Ogletree, K. Watanabe, T. Taniguchi, A. Zettl, and S. Aloni, *Phys. Rev. B* **100**(15), 155419 (2019).
- 26I. Zhigulin, J. Horder, V. Ivády, S. J. U. White, A. Gale, C. Li, C. J. Lobo, M. Toth, I. Aharonovich, and M. Kianinia, *Phys. Rev. Appl.* **19**(4), 044011 (2023).
- 27A. Gale, C. Li, Y. Chen, K. Watanabe, T. Taniguchi, I. Aharonovich, and M. Toth, *ACS Photonics* **9**(6), 2170 (2022).

- ²⁸M. Onodera, M. Isayama, T. Taniguchi, K. Watanabe, S. Masubuchi, R. Moriya, T. Haga, Y. Fujimoto, S. Saito, and T. Machida, *Carbon* **167**, 785 (2020).
- ²⁹H. Akbari, W.-H. Lin, B. Vest, P. K. Jha, and H. A. Atwater, *Phys. Rev. Appl.* **15**(1), 014036 (2021).
- ³⁰N. Mendelson, D. Chugh, J. R. Reimers, T. S. Cheng, A. Gottscholl, H. Long, C. J. Mellor, A. Zettl, V. Dyakonov, P. H. Beton, S. V. Novikov, C. Jagadish, H. H. Tan, M. J. Ford, M. Toth, C. Bradac, and I. Aharonovich, *Nat. Mater.* **20**(3), 321 (2021).
- ³¹C. Lyu, Y. Zhu, P. Gu, J. Qiao, K. Watanabe, T. Taniguchi, and Y. Ye, *Appl. Phys. Lett.* **117**(24), 244002 (2020).
- ³²M. Fischer, J. M. Caridad, A. Sajid, S. Ghaderzadeh, M. Ghorbani-Asl, L. Gammelgaard, P. Bøggild, K. S. Thygesen, A. V. Krasheninnikov, S. Xiao, M. Wubs, and N. Stenger, *Sci. Adv.* **7**(8), eabe7138 (2021).
- ³³M. Koperski, D. Vaclavkova, K. Watanabe, T. Taniguchi, K. S. Novoselov, and M. Potemski, *Proc. Natl. Acad. Sci. U. S. A.* **117**, 13214 (2020).
- ³⁴P. Khatri, A. J. Ramsay, R. N. E. Malein, H. M. H. Chong, and I. J. Luxmoore, *Nano Lett.* **20**(6), 4256 (2020).
- ³⁵M. K. Boll, I. P. Radko, A. Huck, and U. L. Andersen, *Opt. Express* **28**(5), 7475 (2020).
- ³⁶N. Chejanovsky, M. Rezai, F. Paolucci, Y. Kim, T. Rendler, W. Rouabeh, F. Fávoro de Oliveira, P. Herlinger, A. Denisenko, S. Yang, I. Gerhardt, A. Finkler, J. H. Smet, and J. Wrachtrup, *Nano Lett.* **16**(11), 7037 (2016).
- ³⁷G. I. López-Morales, M. Li, A. Hampel, S. Satapathy, N. V. Proscia, H. Jayakumar, A. Lozovoi, D. Pagliero, G. E. Lopez, V. M. Menon, J. Flick, and C. A. Meriles, *Opt. Mater. Express* **11**(10), 3478 (2021).